Cycling test of liquid sorption thermal energy storage using sodium hydroxide

Benjamin Fumey[1], Robert Weber[1] and Luca Baldini[1]

[1] Empa, Dübendorf (Switzerland)

Abstract

In this paper results of an absorption heat storage cycling test are presented. The specific application is long term heat storage, the test setup is based on a spiral finned tube heat and mass exchanger constructed of stainless steel type 1.4571 and the absorbent working pair is sodium hydroxide and water. A total of 7 cycles are performed at approximately 13.5 hours of absorption and 17 hours of desorption time per cycle. Average concentration of sodium hydroxide in the solution is 48 wt% after desorption and 27 wt% after absorption. Comparison of thermal performance among different cycles is made. No clear tendency of cycling improvement or degradation is found.

Keywords: Absorption heat storage, Long term thermal energy storage, Sodium hydroxide / Water, Cycling test, Spiral finned tube heat and mass exchanger

1. Introduction

Heat storage based on sorption process has the prospective for compact thermal storage without suffering loss during storage time. Much research has been done towards this goal, accompanied by several IEA Technology Collaboration Programs [van Helden et al. 2015]. Sorption heat storage operates as a chemically driven heat pump, storing not heat, but the potential to regain heat at elevated temperatures. Applied sorption materials are generally categorized into adsorbents referring to solid sorbents and absorbents referring to liquid sorbents. Categorization is made from an application perspective whereby the sorbate, frequently taken to be water, adheres to the surface of solids and diffuses into liquids. Theoretical work on absorption materials shows promising potential for heat storage application [Hui, et al. 2011], and is seen to have good potential for building integrated heat storage [N'Tsoukpoe, et al. 2009, Tatsidjodoung, et al. 2013, Zhang, et al. 2014]. Common absorbents considered are the aqueous salts lithium bromide (LiBr) [N'Tsoukpoe et al. 2013, Mortazavi et al. 2015], lithium chloride (LiCl) [Bales et al. 2008], calcium chloride ($CaCl_2$) [Quinnell, et al. 2011, Le Pierrès, et al. 2011] and sodium hydroxide (NaOH) [Weber and Dorer, 2008]. First heat storage prototypes for solar heating have been built based on the conventional falling film tube bundle heat and mass exchanger (HMX) [N'Tsoukpoe et al. 2013, Fumey et al. 2015a]. Nevertheless, various issues related to the required large concentration difference in a single cycle process have led to poor operation results. Challenges include regrouping of droplets due to high viscosity of the absorbent working pair as well as high surface tension and high contact angle. Thus, system performance has generally been unsatisfactory, and it is recognized that new HMX concepts are required [N'Tsoukpoe et al. 2013, Daguenet-Frick, et al. 2017]. In contrast to solar sorption chilling machines [Ibarra-Bahena and Rosenberg, 2014] not cold, but heat is sought and not a full cycle but a time interrupted process is at hand. Absorption heat storage performance is measured in respect to energy density and temperature lift [Fumey et al. 2015b]. Energy density is dependent on the degree of absorbate difference between charged and discharged absorbent working fluid and temperature lift is dependent on the concentration of absorbent in the working fluid. High concentration leads to increased temperature lift. A HMX for absorption heat storage must reach maximum absorbate uptake in a single pass process in order to prevent temperature drop due to concentration reduction through mixing of charged absorbent solution with semi discharged solution. Experiments have shown that substantially more exposure time of absorbent solution to absorbate is required then commonly possible in absorption chiller type HMXs [Fumey et al, 2017]. Alternative HMX designs are suggested by [Michel et al. 2017] and [Fumey et al, 2017].

doi:10.18086/swc.2017.13.05 Available at http://proceedings.ises.org

In this paper the cycling test results of a spiral finned tube HMX design as described in [Fumey et al., 2017] made of stainless steel type 1.4571 and operated with aqueous NaOH are presented and compared in respect to important performance parameters with focus on possible degradation.

2. Setup description

In this absorption process, HMX operation is under exclusion of non-condensing gasses. Fig. 1b shows the finned tube heat exchanger used both as absorber and desorber (A/D) as well as evaporator and condenser (E/C). Dual function is possible due to the time separated processes of evaporation and absorption and the process of desorption and condensation. Both, in absorption and desorption operation, aqueous NaOH is introduced to the top of the A/D spiral fin and flows down, channeled along the fin as illustrated in Fig. 1a. In absorption mode, water follows the same principle on the E/C unit whereby it is evaporated by means of low temperature heat source and in turn absorbed on the aqueous NaOH. The heat of vapor condensation as well as to a smaller part the heat of dilution is released at concentration dependent elevated temperature to the heat transfer fluid (HTF). In desorption mode the revers process is followed; heat from the HTF is released to the absorbent, whereby water is evaporated from the aqueous NaOH solution. The water vapor is in turn condensed on the E/C unit and the heat released to the respective HTF. Depending on the NaOH concentration and the temperature difference between A/D and E/C unit absorption or desorption takes place.

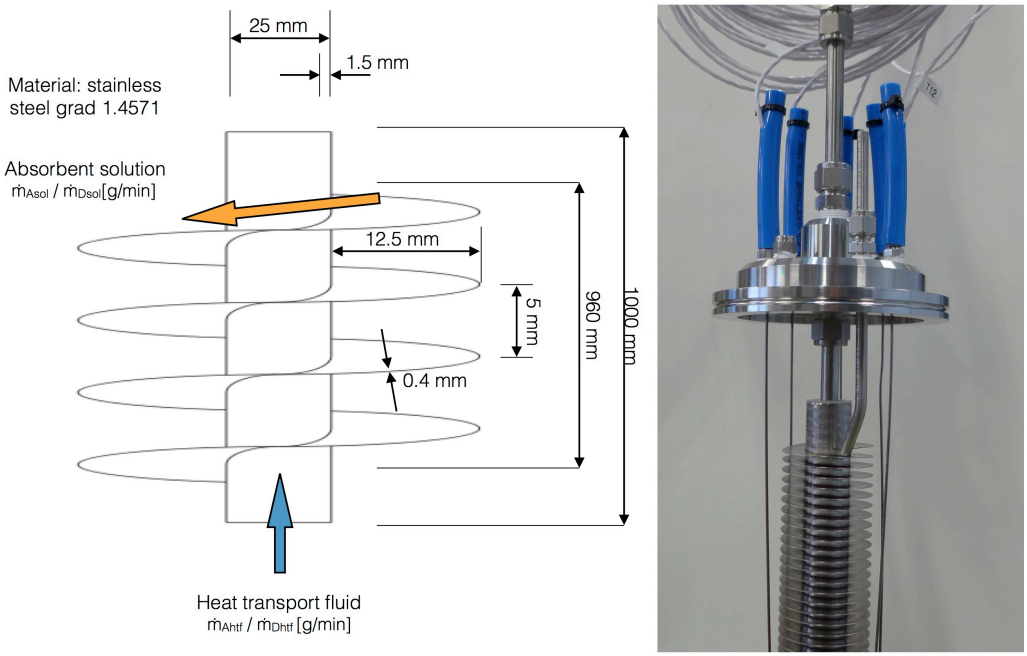

Fig. 1: a) Illustration of the finned tube heat exchanger with absorbent solution flow indicated by the orange arrow and HTF by the blue arrow (left). b) Finned tube heat exchanger showing the sorbent supply tube on the top most fin as well as installed temperature sensors. The HTF flows through the center tube (right).

The benefits of the spiral finned tube heat exchanger are, the long exposure time, large surface area, slow flow of the absorbent and resulting thin film, adjustability of exposure time, film thickness control by absorbent flow regulation, and continuous process both in absorption as well as desorption.

In the lab scale HMX test facility, two spiral finned tubes as A/D and E/C units are installed in two separate chambers respectively as shown in Fig. 2. The two chambers are interconnected in order to enable water vapour exchange and the HMXs are supplied with heat and cold from two thermostat/cryostat baths. These operate as solar heat source and ambient heat sink in desorption also referred to as charging mode as well as low temperature heat source and building heat demand in absorption or discharging mode. Gear pumps circulate the heat transfer fluids, supplied to the bottom of the HMX, in counter flow to the absorbent and absorbate and flow is regulated with buoyancy flow regulators. Both absorbent and absorbate are sourced from plastic canisters at atmospheric pressure. The containers are seen in Fig. 2 at the bottom center. The blue canister holds the absorbent (aqueous NaOH) and the white canister holds the absorbate (water). This is strongly in contrast to the

conventional approach in closed sorption systems where both sorbent and sorbate are stored under low pressure conditions with removal of all non-condensing gasses. Absorbent is dosed to the absorber by a tubing pump seen above the blue canister. Mass flow is monitored by electronic scale placed underneath the absorbent canister. Absorbate is supplied to the E/C chamber from the respective canister by pressure difference between the ambient to the low pressure in the chamber and re-circulated on the HMX using a gear pump. Both absorbent and absorbate are removed from the low pressure HMX chambers by vacuum lock. These consist of a container each connected to the respective chamber via ball valve. The absorber / desorber vacuum lock is indicted in Fig. 2 bottom left. Absorbent and absorbate flows from the HMX into the vacuum lock by gravitational force. Periodically, the interconnecting valves are closed, the lock aired and the working fluids released to plastic container. Prior to opening the valve again, the lock is evacuated. This setup enables periodic sampling without interrupting the continuous operation. Detailed results of initial operation tests are presented in [Fumey et al. 2017].

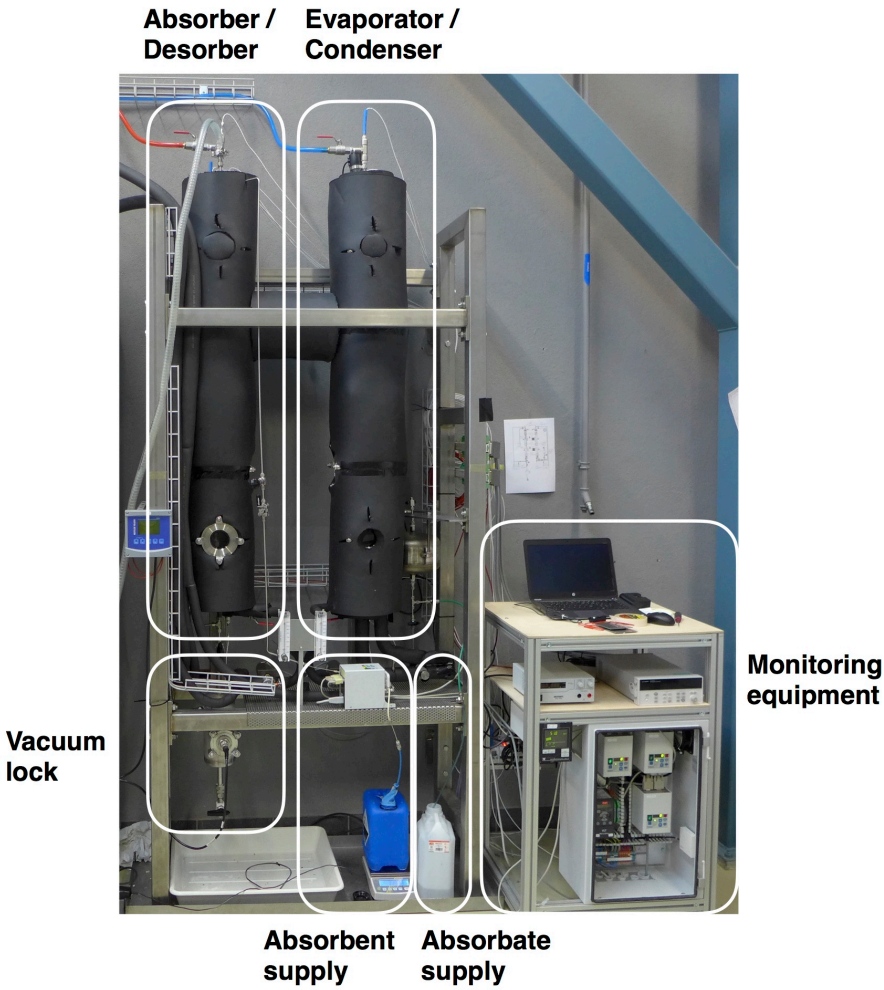

Fig. 2: Test setup including the absorber / desorber composition on the left top, the evaporator / condenser unit on the right top, the absorbent vacuum lock on the left bottom, the absorbent and absorbate supply on the bottom center and the monitoring equipment to the bottom right.

3. Testing procedure

Seven absorption and desorption cycles are undertaken in the described setup and performance is compared in terms of deviation of effective temperature difference from the theoretical temperature difference for a given absorbent concentration. Theoretical values are represented by the equilibrium curve (see Fig. 3-6). This test distinguishes itself from the former tests reported in that both absorbent solution and absorbate are continuously reused. This approach leads to a dependence of absorption performance on the preceding desorption process and

may lead to an accumulation of possible performance depredators. In absorption, the absorbent flow is 6 g/min, the A/D HTF supply temperature is 28 °C at a flow of 200 g/min and the E/C supply temperature is 25°C at a flow of 800 g/min. In desorption the absorbent flow is 8 g/min, the A/D HTF supply temperature is 65 °C at a flow of 800 g/min and the E/C supply temperature is 10 °C at a flow of 1200 g/min. The test duration for a single cycle in absorption is approximately 13.5 hours and the desorption duration is 17 hours due to the greater mass of diluted aqueous NaOH to be transported. One complete absorption and desorption cycle is tested per week resulting in a total test duration of 7 weeks. No absorbent or absorbate is added or removed from the solution during the test series. Both absorbent and absorbate are stored under atmospheric pressure and exposed to air.

4. Results and discussion

Fig. 3 shows the process performance with reference to the ideal equilibrium state of the cycling test with temperature difference between the A/D and E/C unit on the x-axis and the absorbent concentration on the y-axis. Average values of the cycles are shown. The dashed line shows the theoretical equilibrium between the temperature difference and the concentration. In Fig. 3 the red x values show the maximum temperature difference between the absorbent and evaporation temperature during absorption in dependence of the concentration. Due to the varying concentration in the cycling tests, the maximum absorption temperature varies. Performance is measured in dependence of horizontal distance from the equilibrium line. The red + values show the final resulting concentration in the absorption process plotted against the minimum temperature difference between A/D and E/C HMX. As with the x values, performance is measured in dependence of horizontal distance to the equilibrium. Closer fit to the equilibrium line shows good performance in terms of effective mass transfer. The blue o values show the resulting concentration of the desorption cycles. As with the absorption results, close fit to the equilibrium line is desired.

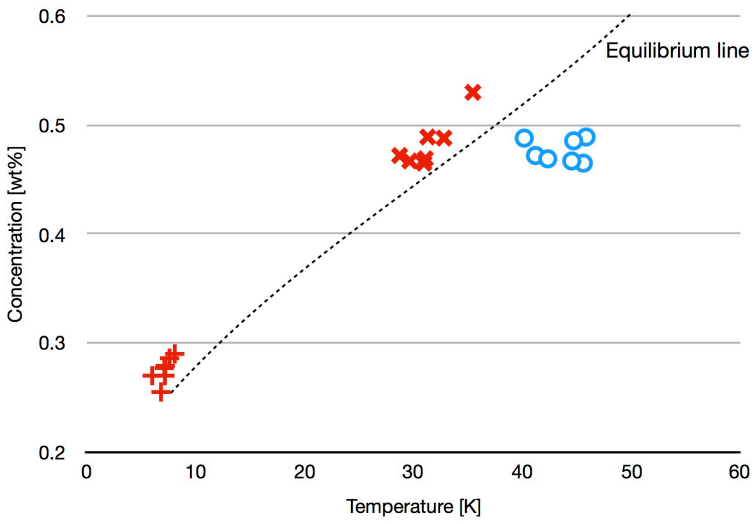

Fig. 3: Overview of resulting concentration/temperature difference pairs recorded during cycle testing in absorption and desorption mode. Red x representing beginning of absorption, red + end of absorption and blue o end of desorption (beginning of desorption is omitted as initial absorbent concentration do not correspond to charging temperatures).

Fig. 4 to 6 show details of the results presented in Fig. 3 for the different operation regimes, beginning and end of absorption as well as end of desorption process, with indication of cycle number for analysis of cycling performance and standard deviation. Fig. 4 shows the maximum temperature increase in respect to concentration in absorption. As expected the temperatures are lower than the equilibrium. Part of this temperature drop is due to water vapor mass diffusion resistance in evaporation, as well as vapor transport from A/D unit to E/C unit and diffusion into the absorbent. It is yet unclear what portion of the total temperature drop is due to this effect.

Test A1 shows a substantially higher temperature gain due to the starting concentration of 53 wt%, temperature increase is directly dependent on absorbent concentration. Nevertheless, it also shoes a large temperature deviation from equilibrium. Interesting is to note that the first 3 cycles have a stronger temperature deviation than the following 4 cycles. Nevertheless, there is no clear tendency observed, highlighting a potential effect of cycling. The least temperature difference is seen at test A5, with tests A6 and A7 showing again an increase. The dashed line is parallel to the equilibrium line with a temperature offset of 4 K representing an average temperature deviation from equilibrium through the set of cycles.

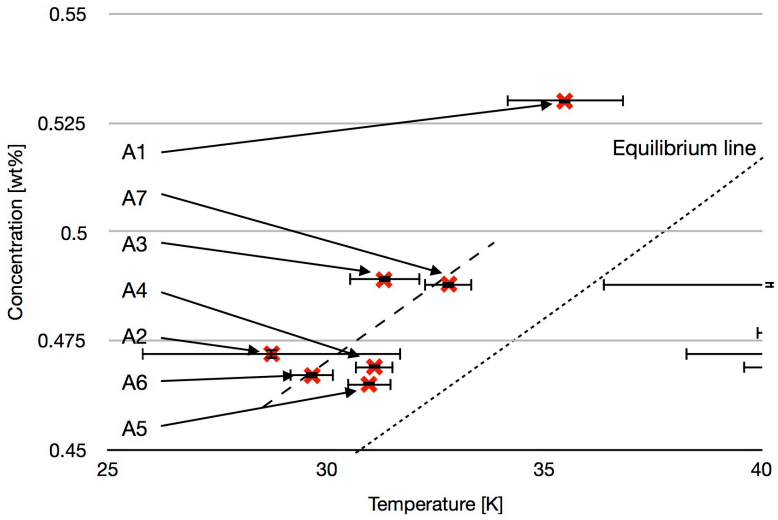

Fig. 4: Focus of Fig. 3 on the maximum temperature increase in respect to the concentration in the absorption process. All values are numbered according to their cycle. The dashed line shows a 4 K offset to the equilibrium line.

Fig. 5 shows the resulting concentration in respect to the minimum temperature difference between the absorber and the evaporator. This is approximately 7 K. As in Fig. 4 there is no trend of degradation or improvement visible across the cycles. Apart from cycle A1 and A6, all results show approximately the same offset to the equilibrium line of approximately 3 K as indicated by the dashed line parallel to the equilibrium line. The concentration difference results from the slightly varying temperature difference between the cycles.

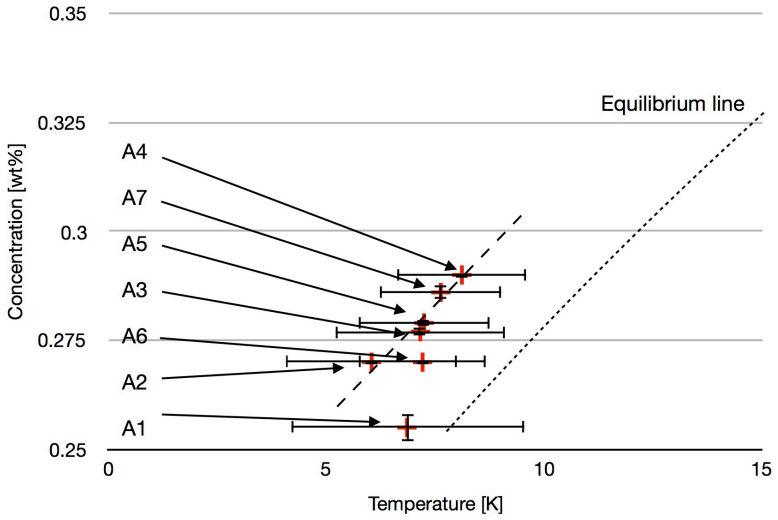

Fig. 5: Focus of Fig. 3 on the minimum concentration reached in absorption modus. All values are numbered according to their cycle. The dashed line shows a 3 K offset to the equilibrium line.

Fig. 6 shows a close up of the resulting concentration in respect to the temperature difference in the desorption process. Compared to the absorption results in figures 4 and 5 there is a greater average deviation from the equilibrium line in the desorption process. It appears that more time is required in order to reach a closer fit to

the equilibrium line. As in absorption, mass transport resistance is three fold; desorption, vapor transport and condensation. Assuming that vapor transport resistance and water phase change on the E/C unit is equal in the absorption as well as the desorption process, it may be concluded that there is a greater mass transport resistance in desorption than in absorption. The dashed line shows an offset of 9 K. As for absorption, there is no clear degradation trend to be recognized in desorption.

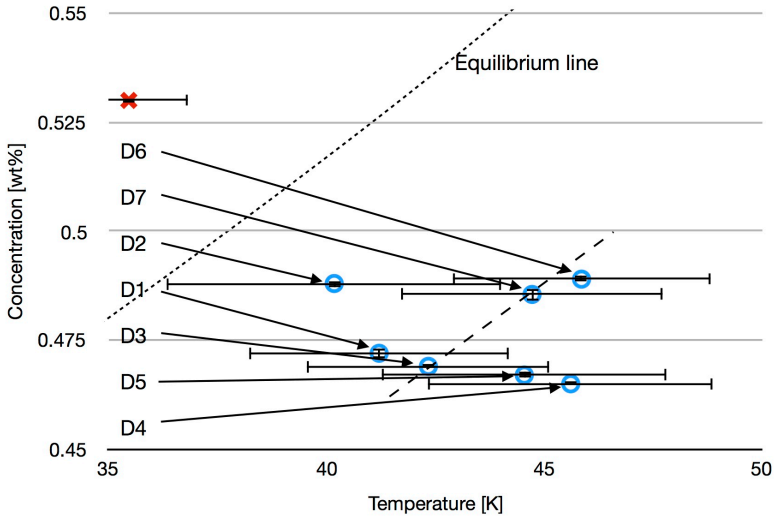

Fig. 6: Focus of Fig. 3 on the maximum concentration reached in desorption modus. All values are numbered according to their cycle. The dashed line shows the 9 K offset to the equilibrium line.

From the illustrated results it is shown that in respect to performance there is no clear trend of degradation or improvement.

It can be seen that even though both absorbent and absorbate are exposed to air in storage, no performance loss is encountered. On a system level this is a very important result, due to the large potential of system simplification and reduction of component costs.

5. Conclusion and outlook

In this paper a cycling test of 7 cycles is presented based on a spiral finned tube heat and mass exchanger for absorption heat storage. Results show good cycling stability without any clear degradation of the process. Storage of both absorbent and absorbate at ambient pressure is seen to be a promising approach for substantial reduction of system complexity and cost. Further work will include measurement over increased number of cycles with chemical analysis of absorbent in between the cycles.

6. Acknowledgements

We gratefully acknowledge financial support by the Swiss Comission for Technology and Innovation (CTI) through the Swiss Competence Center for Energy Research Heat and Electricity Storage.

7. References

B. Fumey, R. Weber, L. Baldini, 2017, Liquid sorption heat storage – A proof of concept based on lab measurements with a novel spiral fined heat and mass exchanger design, In Applied Energy, Volume 200, Pages 215-225,

Bales C., 2008, Final report of subtask B chemical and sorption storage the over- view, Available from: http://archive.iea-shc.org/publications/ downloads/task32-b7.pdf

Benjamin Fumey, Robert Weber, Paul Gantenbein, Xavier Daguenet-Frick, Ian Hughes, Viktor Dorer, 2015b, Limitations Imposed on Energy Density of Sorption Materials in Seasonal Thermal Storage Systems, In Energy Procedia, Volume 70, Pages 203-208,

Benoit Michel, Nolwenn Le Pierrès, Benoit Stutz, 2017, Performances of grooved plates falling film absorber, In Energy, Volume 138, 2017, Pages 103-117,

Fumey B., Weber R., Gantenbein P., Daguenet-Frick X., Stoller S., Fricker R., Dorer V., 2015a, Operation Results of a Closed Sorption Heat Storage Prototype, Energy Procedia, Volume 73, 324-330

Jonathan Ibarra-Bahena and Rosenberg J. Romero, 2014, Performance of Different Experimental Absorber Designs in Absorption Heat Pump Cycle Technologies: A Review, Energies, 7, 751-766

K. Edem N'Tsoukpoe, Hui Liu, Nolwenn Le Pierrès, Lingai Luo, 2009, A review on long-term sorption solar energy storage, In Renewable and Sustainable Energy Reviews, Volume 13, Issue 9, Pages 2385-2396

K.E. N'Tsoukpoe, N. Le Pierrès, L. Luo, 2013, Experimentation of a LiBr–H2O absorption process for long-term solar thermal storage: Prototype design and first results, In Energy, Volume 53, Pages 179-198,

Le Pierrès N., Liu H., Luo L., 2011, CaCl2/H2O absorption seasonal storage of solar heat, Proceedings of the international conference for sustainable energy storage, Belfast, Ulster, Feb 21-25.

Liu Hui, N'Tsoukpoe K. Edem, Le Pierres Nolwenn, Luo Lingai, 2011, Evaluation of a seasonal storage system of solar energy for house heating using different absorption couples, In Energy Conversion and Management, Volume 52, Issue 6, 2011, Pages 2427-2436,

Mehdi Mortazavi, Rasool Nasr Isfahani, Sajjad Bigham, Saeed Moghaddam, 2015, Absorption characteristics of falling film LiBr (lithium bromide) solution over a finned structure, In Energy, Volume 87, Pages 270-278

Parfait Tatsidjodoung, Nolwenn Le Pierrès, Lingai Luo, 2013, A review of potential materials for thermal energy storage in building applications, In Renewable and Sustainable Energy Reviews, Volume 18, Pages 327-349

Quinnell J.A., Davidson J.H., Burch J. 2011, Liquid calcium chloride solar storage: concept and analysis, Journal of Solar Energy Engineering.

R. Weber, V. Dorer, 2008, Long-term heat storage with NaOH, In Vacuum, Volume 82, Issue 7, Pages 708-716

Wim van Helden, Motoi Yamaha, Christoph Rathgeber, Andreas Hauer, Fredy Huaylla, Nolwenn Le Pierrès, Benoit Stutz, Barbara Mette, Pablo Dolado, Ana Lazaro, Javier Mazo, Mark Dannemand, Simon Furbo, Alvaro Campos-Celador, Gonzalo Diarce, Ruud Cuypers, Andreas König-Haagen, Stephan Höhlein, Dieter Brüggemann, Benjamin Fumey, Robert Weber, Rebekka Köll, Waldemar Wagner, Xavier Daguenet-Frick, Paul Gantenbein, Frédéric Kuznik, 2016, IEA SHC Task 42 / ECES Annex 29 – Working Group B: Applications of Compact Thermal Energy Storage, In Energy Procedia, Volume 91, Pages 231-245,

Xavier Daguenet-Frick, Paul Gantenbein, Jonas Müller, Benjamin Fumey, Robert Weber, 2017, Seasonal thermochemical energy storage: Comparison of the experimental results with the modelling of the falling film tube bundle heat and mass exchanger unit, In Renewable Energy, Volume 110, Pages 162-173,

Xiaoling Zhang, Minzhi Li, Wenxing Shi, Baolong Wang, Xianting Li, 2014, Experimental investigation on charging and discharging performance of absorption thermal energy storage system, In Energy Conversion and Management, Volume 85, Pages 425-434